Fast Line and Object Segmentation in Noisy and Cluttered Environments using Relative Connectivity

Michael Teutsch[1] and Thomas Schamm[2]
[1]Fraunhofer IOSB, 76131 Karlsruhe, Germany, Email: michael.teutsch@iosb.fraunhofer.de
[2]FZI Forschungszentrum Informatik, 76131 Karlsruhe, Germany, Email: schamm@fzi.de

Abstract— *In applications such as 3D plane segmentation of road traffic environments using u/v-disparity-histograms, line extraction is a key component and has to be as fast and precise as possible. Hough Transform is a good way to detect straight lines but specific line segments limited by start and end points are still to be determined. The* Line Patterns Hough Transform (LPHT) *introduced by Yip[1] directly delivers potential start and end points using the principle of relative connectivity. But this approach poses some challenges, too. We modified his idea to use Standard Hough Transform (SHT) together with relative connectivity for a fast and robust line segment extraction even in environments strongly affected by noise and clutter. Furthermore, we demonstrate the benefit of modified LPHT and relative connectivity for object segmentation in noisy Synthetic Aperture Radar (SAR) or infrared (IR) data.*

Keywords: Line Patterns Hough Transform, LPHT, line detection, line extraction, foreground background segmentation.

1. Introduction

The Standard Hough Transform (SHT) [2], [3] is a widely spread method for line segmentation due to its easy implementation and good performance. It has some drawbacks such as the slow computation time or high memory requirements. Over the years, several variations like the Fast Hough Transform or the Randomized Hough Transform were introduced to handle these problems. But there are also some other demanding challenges:

1) Similarity: Maxima in the Hough accumulator close to each other lead to similar straight lines.
2) Connectivity: Collinear and contiguous points create maxima in Hough accumulator space, but maybe are not part of the same line segment [3].
3) Start/Endpoints: Maxima in Hough accumulator represent straight lines. If line segments are desired, they have to be extracted subsequently.

In his work, Yip [1] deals with all five mentioned problems including computation time and memory requirements, but with a more detailed discussion on the latter three. He proposes a modified Hough Transform, namely the *Line Patterns Hough Transform (LPHT)*, to directly extract potential start and end points of line segments. Therefore, he uses the principle of *relative connectivity* of points along a line segment instead of straight lines. Relative connectivity is defined as "the relationship of a set of collinear and equidistant points with regard to contiguity" [1]. The benefits and problems of his idea will be shown and discussed in section 2.

With the LPHT, start and end points of areas with strong relative connectivity can be found. However, these start and end points are not yet combined to line segments. Thus, the assignment of start to end points is a sophisticated topic within the LPHT with no straightforward standard solution. In our application of 3D plane segmentation, where fast and precise line segmentation in u-/v-disparity-histograms is the main challenge, this assignment appeared to be difficult and not reliable. In section 4 we present a way to use modified LPHT with regards to relative connectivity in combination with the SHT to get accurate line segments in real-time facing the three mentioned problems. This approach has been successfully applied for line segment extraction in [4] and [5], but the segmentation process was not described in detail and, hence, will be the focus of this paper.

In further experiments, we discovered that the principle of relative connectivity without SHT is also suitable for object segmentation and performs well especially in highly noisy and cluttered environments. Synthetic Aperture Radar (SAR) or infrared (IR) data often suffers from strong speckle noise. Additionally, SAR data has several more characteristics, which make precise object segmentation difficult. We demonstrate the profit of using the modified LPHT to segment ships in TerraSAR-X satellite images for maritime surveillance. Some background information about TerraSAR-X data processing can be found in [6].

Related work

We divide the related work in two topics: Line segment extraction based on Hough Transform and object segmentation in IR or SAR image.

Standard Hough accumulator space has two dimensions: Straight line slope and offset. In [7], line segments are extracted by extending the Standard Hough accumulator to a three-dimensional space considering the image's x-axis as spatial information, too. Detected maxima in 3D Hough space correspond to straight lines with already known range in x-direction for the related line segment. Thus, the line segment can be cut out from the straight line. In [8], the Connectivity Weighted Hough Transform (CWHT) is introduced: Connectivity between two points is calculated by the number of edge points divided by the number of non-edge points lying on the line segment between them. This connectivity is used as weight for the entry of these two points to the accumulator of Randomized Hough Transform (RHT). Kamat et al. [9] point out, that maxima in Standard Hough accumulator have butterfly shape. In the area of this butterfly shape, information about start and end point is contained, too. By detecting not only the maximum but also a window area framing the butterfly shape, start and end point can be determined. In [10], a detailed introduction to neighborhood mapping between the input image and the Hough accumulator space is given. It is possible to make a straight line segment neighborhood in the image consistent with a straight line segment neighborhood in the accumulator. In image processing applications, this mapping has to be approximated: A line segment in the image can be represented by a quadrangle in the accumulator space.

For the segmentation of aircraft objects in infrared images, Li et al. [11] use Otsu thresholding, contour tracking and a scan line filling algorithm to get object blobs without disturbing holes and gaps. A combination of Otsu thresholding and Negative Selection algorithm is used in [12] to segment objects with noisy and blurred edges in infrared images. In [13], object segmentation in SAR images is discussed. A Wiener filter is applied to remove speckle noise but preserve edges. In the follow-up, four segmentation techniques are compared to each other with the result that CFAR-like methods and approaches tracing the object boundaries perform best. Refer to [14] for further information about Constant False Alarm Rate (CFAR). In [15], a CFAR-algorithm is applied for initial ship detection in TerraSAR-X images. The combination of row- and column-wise median filtering is used to suppress speckle noise. Finally, an iterative algorithm is executed, evaluating the segmentation quality with convexity measurement of the object blob on the one hand, and trying to maximize this quality on the other. This way, typical SAR blooming effects are suppressed.

This paper provides the following organization: The original LPHT-algorithm is presented in section 2, while the proposed modification is introduced in section 3. Example applications results are demonstrated with line segmentation in section 4 and with object segmentation in section 5. Finally, conclusions are given in section 6.

2. The original LPHT-algorithm

The basic ideas of the original LPHT-algorithm as proposed by Yip [1] are presented in this section. Besides the general concept, a brief description of the principle of relative connectivity is given. With an evaluation and discussion we point out the motivation for our proposed modification.

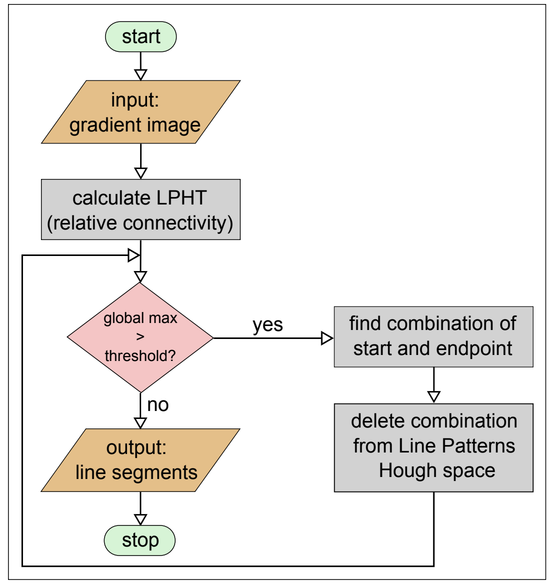

Fig. 1: The concept of the original LPHT-algorithm.

2.1 Concept

The concept is displayed in Fig. 1. Different kinds of input images are possible such as gradient images or *u/v-disparity-histograms* (see section 4). The LPHT uses relative connectivity to emphasize potential start and end point with a high accumulation value in the Line Patterns Hough accumulator. Due to the conceptual design of the LPHT, the spatial dimensions of this accumulator are equal to horizontal and vertical image dimension. Thus, potential start and end points in the accumulator are at the same position as in the input image. This is a difference to the SHT, where the two spatial dimensions of the Hough accumulator are given by the number of discretization steps for potential straight line slopes and offsets. These are for example angle θ and algebraic distance ρ of the normal parameterization $x \cdot \cos\theta + y \cdot \sin\theta = \rho$ proposed by Duda and Hart [3] to be used as straight line representation in SHT.

As long as the highest value in the Line Patterns Hough accumulator exceeds a specific threshold, this peak is interpreted as start point and a well-fitting, related end point is determined. This start and end point combination is then deleted from the accumulator and the next global maximum is searched. Other ways of assigning start and end points are possible as well: Yip [1] proposed to take all local maxima exceeding a specific threshold and perform a kind of multi-hypothesis assignment evaluating all combinations and choosing the best. This might cause big computational effort, so we decided to implement the approach shown in Fig. 1.

2.2 Accumulated relative connectivity

Principal component of the LPTH is the calculation of relative connectivity. Line Patterns Hough accumulator is the result of this calculation emphasizing potential start and end points. High values for relative connectivity are achieved for a set of collinear, equidistant, and contiguous points and subsequently added to the accumulator.

For the algorithm description, we closely follow the connectivity theory of Duda and Hart [3], and Yip [1]. The algorithm to calculate accumulated relative connectivity is shown as pseudo-code in [1]. The input image is scanned pixel by pixel in vertical and horizontal direction for points potentially belonging to a line segment. If pixel intensity $I(x, y)$ at image position (x, y) exceeds a specific intensity threshold t, the pixel is considered for this belonging. This leads to the binary belonging function B:

$$B(x, y) = \begin{cases} 1, & \text{if } I(x, y) \geq t \\ 0, & \text{if } I(x, y) < t. \end{cases}$$

For a set of collinear and equidistant points $P_i(x_i, y_i)$ with $i \in \{1, \ldots, n\}$ and $\forall i$: $B(x_i, y_i) = 1$, the relative displacement $(\Delta x, \Delta y)$ is given by

$$\begin{aligned} \Delta x &= x_2 - x_1 \\ \Delta y &= y_2 - y_1. \end{aligned}$$

For being a start point, P_1 has to satisfy the constraint

$$B(x_1, y_1) = 1 \qquad \text{and} \qquad B(x_1 - \Delta x, y_1 - \Delta y) = 0.$$

The definition of P_n being an end point is done analogously

$$B(x_n, y_n) = 1 \qquad \text{and} \qquad B(x_n + \Delta x, y_n + \Delta y) = 0.$$

n is the connectivity number, since

$$B(x_n + \Delta x, y_n + \Delta y) = B(x_1 + n \cdot \Delta x, y_1 + n \cdot \Delta y) = 0$$

and

$$B(x_1 + i \cdot \Delta x, y_1 + i \cdot \Delta y) = 1 \qquad \forall i \in \{0, \ldots, n-1\}.$$

To store this found relative connectivity, n is entered to the Line Patterns Hough accumulator at start and end point position (x_1, y_1) and (x_n, y_n).

2.3 Discussion

A big set of consecutive equidistant and collinear points causes high accumulation values. Since the considered relative displacement Δ between points is gradually incremented during processing, small gaps in the input data can be handled when Δ gets bigger. This makes the approach robust even in noisy and cluttered environments. But considered relative displacement has to be limited by a maximum threshold Δ_{max} to avoid noise in the accumulator. Weak relative connectivity caused by small connectivity number n causes noise in the accumulator, too, but can be suppressed easily by the accumulation constraint $n > m$ with m being the threshold for minimum accumulation. Three parameters are affecting the quality of the relative connectivity strongly:

1) Intensity threshold t:
   This is the most important parameter as it is actuating the number of potential line segment points.
2) Maximum relative displacement Δ_{max}:
   As already mentioned, this parameter is used to avoid split line segments. On the other hand, it can cause merged line segments, if it is getting too big. Thus, Δ_{max} should be chosen small in case of weak noise and bigger for strong noise.
3) Minimum accumulation threshold m:
   In our experiments, we simply set $m = 2$, because we worked on noisy data and wanted to keep all available connectivity information.

The estimated complexity for calculating relative connectivity with this algorithm is $O(M \cdot N \cdot \log M \cdot \log N)$ for an input image of size $M \times N$. The computational effort is closely related to the number of potential line segment points. Major problem of the LPHT is the assignment of related start and end points. In input images, where many line segments are expected, the assignment of start and end points can lead to confusion and high computation time. However, SHT will be harmed in that case either. But with our modification, we found a way to handle such situations.

3. The proposed modification

In the original algorithm for accumulated relative connectivity, two-dimensional input images are processed, while in our modification one-dimensional *coverage histograms* coming from the SHT are considered. Thus, main component of our modification is the combination of SHT and LPHT to benefit from their advantages: Getting straight lines but no start/end points from SHT and getting start/end points without danger of confusion in 2D Line Patterns Hough accumulator from LPHT. This way, not only the computation time is reduced, but also the assignment of start and end points is easier.

3.1 Concept

In Fig. 2, the concept of our modification is shown. SHT is used to calculate the Standard Hough accumulator of the input image. If the global maximum exceeds a specific threshold, the related straight line is considered for the further steps: A coverage histogram is initialized, where the number of bins is equal to the length of the straight line. For each point of the straight line a coverage area in the input image is scanned and for each found, *covered* point, the related histogram bin is incremented. Fig. 4 shows the idea of covered points and coverage area (ϵ region in red).

Now, the LPHT is calculated only for this coverage histogram. Just the two highest accumulation values (maxima) are taken as start and end point for the line segment. In a final step, the covered points in the input image are deleted from the Standard Hough accumulator to avoid the problems of similarity and connectivity for the next cycle.

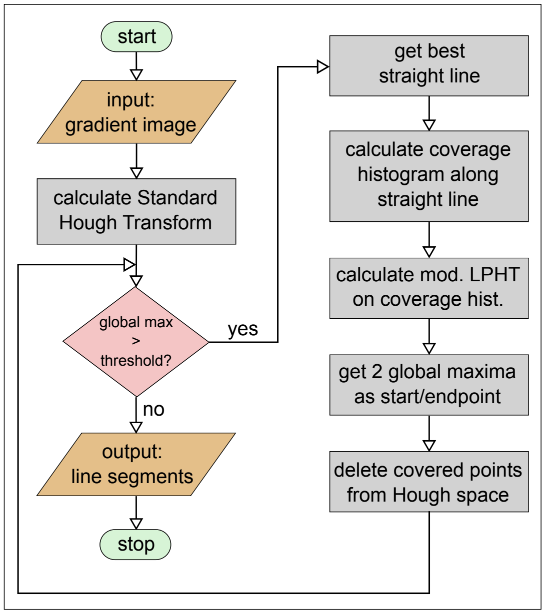

Fig. 2: The concept of the modified LPHT-algorithm in combination with SHT.

3.2 Modified LPHT and discussion

The modified algorithm for calculation of accumulated relative connectivity is presented as pseudo-code in algorithm 1. While the original algorithm was processing two-dimensional input images, the modified version works on one-dimensional input arrays such as coverage histograms. Hence, the Line Patterns Hough accumulator is much smaller as in the original algorithm, since it has the same size as the coverage histogram. The complexity has been reduced to $O(N \cdot \log N)$ with N being the number of bins in the histogram. Furthermore, the search for fitting start and end points has been reduced from 2D to a 1D search problem.

The computational effort for calculating the SHT to get the best straight line is comparable to the LPHT without start/end point assignment. But determining line segments in coverage histograms is much easier and faster than in the input image even with respect to deletion of covered points from the Standard Hough accumulator.

With our proposed modification it is possible to get precise line segments in real-time even when processing input data severely affected by noise. Some examples are given in the following sections about applications.

4. Line segmentation

The proposed modification of LPHT will now be used segment 3D planes in point clouds coming from a Time Of Flight (TOF) camera. In most cases, plane segmentation in 3D point clouds under the occurrence of clutter is achieved by considering planes parallel to the image plane only. Therefore, many algorithms filter noisy image data using local homogeneity criterion, as presented in [16]. Other algorithms make usage of 2D image segmentation algorithms to segment depth points, e.g., unseeded region growing [17]. Our presented 3D point cloud segmentation algorithm is more related to stereo image processing, in particular disparity image segmentation using disparity histograms. This approach was first introduced by [18] for road plane extraction. In [19], the proposed method was extended for robust object detection as well. Even in noisy and cluttered environments, these algorithms provide reliable segmentation of planes which are parallel to one of the image plane axes.

An example for disparity histograms is shown in Fig. 3.

Algorithm 1 Modified accumulation of relative connectivity.

/* let H be the coverage histogram */
/* let N be the number of histogram bins */
/* let t be the histogram bin value threshold */
/* let n be the number of found collinear points */
/* let m be the accumulator acceptance threshold */
/* let A be the Line Patterns Hough accumulator */
for x_1 = 1 to N **do**
  if $H(x_1) \geq t$ **then**
    for $x_2 = x_1 + 1$ to $x_1 + \Delta_{max}$ **do**
      if $H(x_2) \geq t$ **then**
        $dx = x_2 - x_1$
        if $H(x_1 - dx) < t$ **then**
          /* found start point */
          $x_n = x_2$
          $n = 2$
          $ready = 0$
          while $ready = 0$ **do**
            if $H(x_1 + dx) \geq t$ **then**
              /* found another line point */
              $n = n + 1$
              $x_n = x_n + dx$
            else
              /* found end point */
              $ready = 1$
            end if
          end while
          if $n \geq m$ **then**
            /* found enough line points */
            /* enter start point to accumulator */
            $A[x_1] = A[x_1] + n$
            /* enter end point to accumulator */
            $A[x_n] = A[x_n] + n$
          end if
        end if
      end if
    end for
  end if
end for

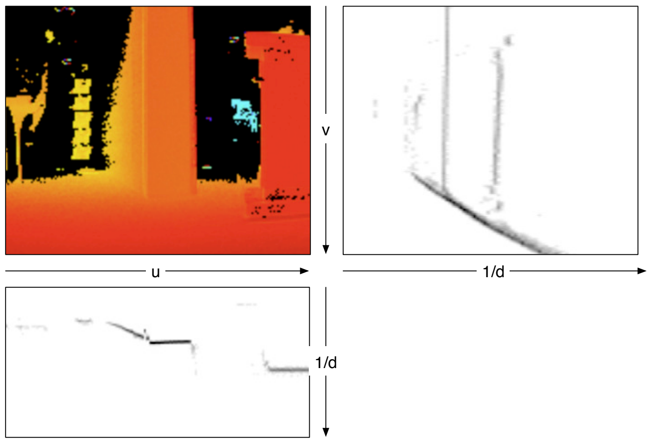

Fig. 3: Color coded range image and corresponding u-/v-histograms. $1/d$ is the reciprocal distance value.

In the follow-up, we will continue calling them *disparity histograms* as they have been named in the literature, unless we use reciprocal distance values instead of disparities. In the color coded range image, warm colors correspond to near distances and cold colors to far distances. The u-/v-disparity-histograms are generated by considering each pixel in the range image and accumulating its reciprocal distance value in each histogram along the u-/v-axis of the image coordinate system respectively. Thus, the 3D plane segmentation problem can be reduced to a 2D line segmentation problem in the resulting histogram images. Line segmentation is performed for each histogram image respectively. Noise in the range image causes noise in the histograms and potentially leads to undesirably split and merged line segments. With modified LPHT we aim to handle this problem.

4.1 Line segment extraction

Fig. 2 depicts the concept of line segment extraction. With SHT we generate the Hough accumulation space, where the highest values define strong straight lines in the histogram image. The best line segment of the strongest straight line is extracted using proposed 1D LPHT. Afterwards, the histogram pixels covered by the line segment are removed from both the Hough space and the histogram image. The algorithm continues finding and analyzing the next maximum in the Hough space, until a certain abort criterion is satisfied.

4.1.1 Hough Transform

After histogram construction, straight lines must be extracted in both u- and v-disparity-histogram images. Thereby we use SHT. By definition, no vertical lines can exist in the u-disparity-histogram image. So we are able to narrow the Hough space's dimension to search for straight lines only for angular values $\theta = [0 + \epsilon, \pi - \epsilon]$. Likewise, no horizontal lines can exist in the v-disparity-histogram image, so the Hough space dimension is limited to $\theta = \left[-\frac{\pi}{2} + \epsilon, \frac{\pi}{2} - \epsilon\right]$.

The histogram values can be projected directly into the Hough space. By weighting the Hough transform with the histogram's accumulation values, strong points in the histogram cause higher peaks in the Hough space:

$$\rho_u(\theta) = \left(u \cos\theta + \frac{1}{d} \sin\theta\right) \text{acc}\left[u, \frac{1}{d}\right] \quad (1)$$

$$\rho_v(\theta) = \left(\frac{1}{d} \cos\theta + v \sin\theta\right) \text{acc}\left[\frac{1}{d}, v\right] \quad (2)$$

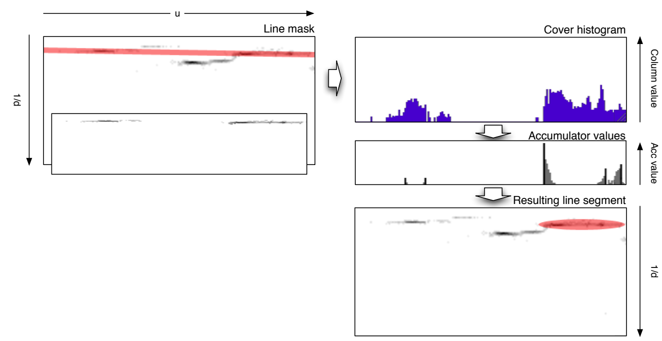

Fig. 4: Line pattern analysis using coverage histogram and modified LPHT.

4.1.2 Line pattern analysis

Maximum values in the calculated Standard Hough spaces correspond to strong lines in the histogram images. By definition, lines given by Hough parameters (ρ, θ) do not have start or end points. Hence, the next step is to extract line segments. For this we calculate the coverage histogram considering only the points in the u-(v-)histogram image matched by the straight line defined by (ρ, θ), and some ϵ region (see Fig. 4).

All values in this ϵ region are accumulated per column (row) in the u-(v-)disparity-histogram image, so that each column (row) along the straight line has its own coverage value. Next, we apply the modified LPHT by calculating relative connectivity along the 1D coverage histogram. In the top left image of Fig. 4, the line mask is shown as a red line, while the three images on the right show the coverage histogram and the calculation of accumulated relative connectivity along the coverage histogram. The red circle marks the resulting line segment.

After line segment extraction, the points belonging to the segment are removed from both the Hough space and the histogram image. This allows the segmentation method to be sensitive even for small but important line segments, as seen in Fig. 5.

The computation time is between 40 and $60\,ms$ for segmentation of all objects in u- and v-disparity-histogram images. The TOF image has a size of 176×144 pixels.

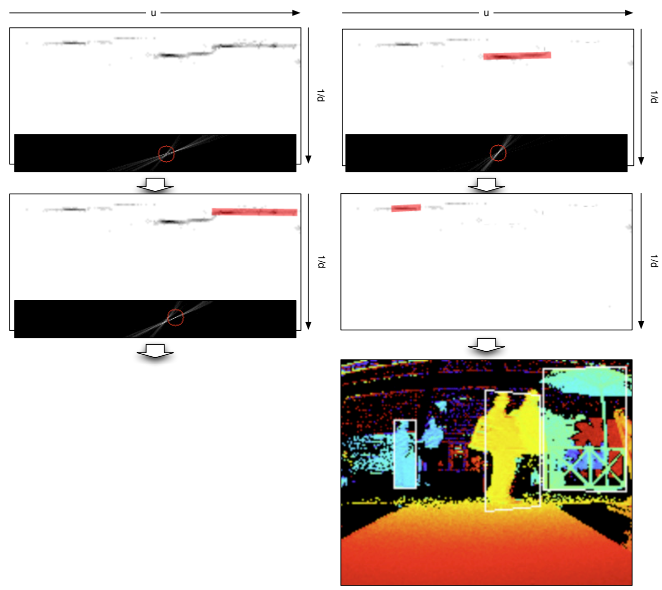

Fig. 5: Extracting and removing line segments from Hough space and histogram image until abort criterion is satisfied.

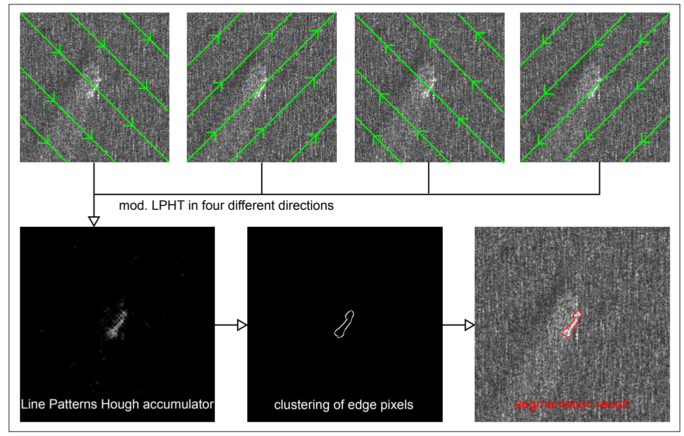

Fig. 6: Scanning the SAR image with modified LPHT.

5. Object segmentation

In the follow-up, we present a method for object segmentation using only the modified LPHT without SHT. We use it to extract contours of maritime objects in TerraSAR-X images. Synthetic Aperture Radar (SAR) is an imaging technique using radar waves. Strong reflections are displayed as high intensity values and weak reflections as low intensity values. Hence, ships appear in the image as bright, elongate blobs. TerraSAR-X is a German satellite giving SAR images in high resolution of up to $1.5 \times 1.5\,m$ per pixel. In our experiments, we used resolution of $3 \times 3\,m$ per pixel. Thus, it is possible to cover a bigger area in one image, which is an important aspect for maritime surveillance. In a first step, object hypotheses are extracted using CFAR algorithm. Each hypothesis is given in the center of a region of interest (ROI) image of 300×300 pixels. They are the input images.

Precise object segmentation is desired to accurately estimate size and orientation of ships. Furthermore, segmentation quality is affecting a subsequent classification step to distinguish between ships and clutter objects significantly as we already found out in [20]. However, it is a difficult task as SAR data is heavily influenced by speckle noise. In addition, object appearance can change very much from image to image depending on many factors such as incidence angle of the sensor, ship orientation, ship motion, ship consistence, and weather. Typical SAR noise effects besides speckle noise are paraxial blooming, smearing, and weak contrast. These effects are shown in the lower row of Fig. 7.

5.1 Proposed segmentation method

Typical speckle noise reduction e.g., by using median filter is not necessary for our approach. The SAR image is scanned row-wise using the modified LPHT-algorithm. Resulting relative connectivity is stored in an accumulator of same size as the input image like in original LPHT. The important intensity threshold parameter t is determined data-driven by using a quantile in the ROI's intensity histogram. This is possible as expected minimum and maximum ship sizes are barely known. By considering each row separately, we aim to find either low relative connectivity in case of no object or high relative connectivity in case of object. Maxima will arise in the area of the object contour even if small gaps exist in the object blob. Scanning is not done horizontally, but diagonally to suppress paraxial blooming. Due to the principle of relative connectivity, ascending intensity values create clear maxima in the accumulator, while descending intensities cause slight smearing. To suppress this effect, row-wise scanning is performed four times diagonally in different directions as demonstrated in Fig. 6. LPHT emphasizes the object structure significantly as seen in the Line Patterns Hough accumulator. For object contour segmentation, it is sufficient now to use a Canny-like edge filter directly on the accumulator and a standard clustering algorithm on the resulting gradient image.

Some examples are shown in Fig. 7, where object segmentation especially in situations of strong noise and clutter is pointed out. The runtime is between 50 and $60\,ms$ per object. For satellite applications this is absolutely suitable.

6. Conclusions

Line Patterns Hough Transform (LPHT) originally proposed by Yip [1] can be used to directly extract potential start and end points of line segments from images. It is using the principle of relative connectivity between line segment points. However, it can be difficult to assign these found start and end points to each other especially in noisy and

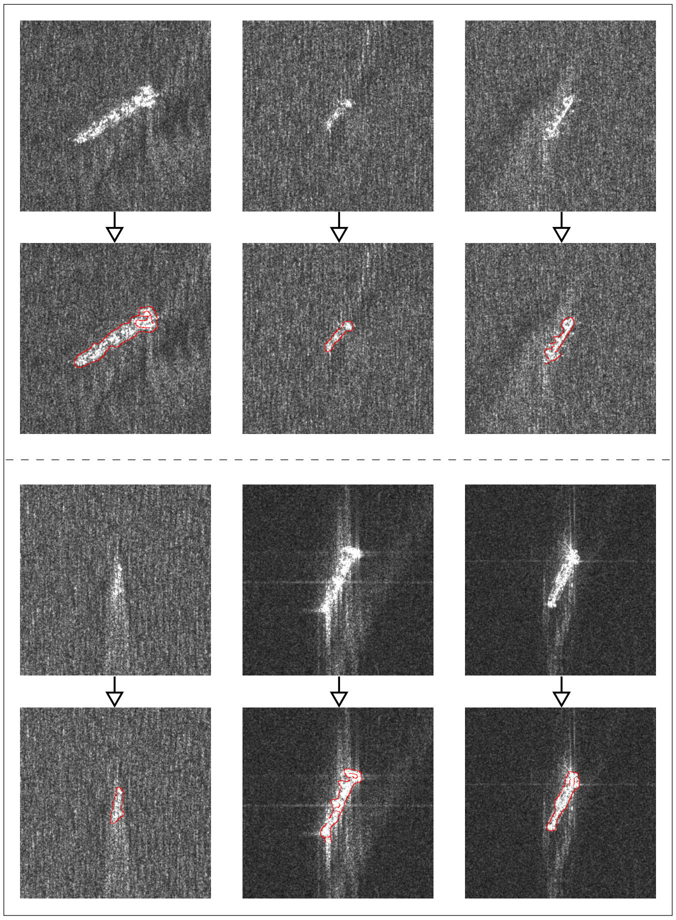

Fig. 7: Examples for object segmentation in noisy and cluttered SAR images using modified LPHT.

cluttered environments. We propose a combination of Standard Hough Transform (SHT) and LPHT. The original LPHT is modified to make it work with reduced complexity, i.e. on one-dimensional coverage histograms. These coverage histograms are calculated along straight lines detected with SHT by accumulating all covered line segment points in an ϵ region. Thus, the problem of start/end point assignment has been reduced significantly. On the same time, relative connectivity makes this approach robust against strong noise and clutter. This is demonstrated in an example application of plane segmentation in 3D point clouds. Furthermore, modified LPHT can be used without SHT for precise object segmentation in noisy SAR and IR data.

Acknowledgement

TOF image segmentation was partially supported by Ministry of Economic Affairs of Baden-Württemberg, Germany. TerraSAR-X segmentation was supported with funds from German Bundesministerium für Wirtschaft und Technologie (BMWi) and DLR Space Agency. The TerraSAR-X images have been provided by DLR and infoterra GmbH.

References

[1] R. K. K. Yip, "Line Patterns Hough Transform for Line Segment Detection", in *Proceedings of the 1994 IEEE Region 10's Ninth Annual International Conference (TENCON'94). Theme: Frontiers of Computer Technology*, pp. 319-323, August 22-26, 1994.

[2] P. V. C. Hough, "Method and Means for Recognizing Complex Patterns", *U.S. Patent 3,069,654*, 1962.

[3] R. O. Duda, P. E. Hart "Use of the Hough Transform to Detect Lines and Curves in Pictures", *Communications of the ACM*, vol. 15, no. 1, January 1972.

[4] M. Teutsch, T. Heger, T. Schamm, J. M. Zöllner, "3D-Segmentation of Traffic Environments with U/V-Disparity supported by Radar-given Masterpoints", in *Proceedings of the 2010 IEEE Intelligent Vehicles Symposium*, San Diego, CA, USA, June 21-24, 2010.

[5] T. Schamm, A. Rönnau, J. M. Zöllner, "Fast 3D Time of Flight Data Segmentation using the U-V-Histogram Approach", in *Proceedings of the Third International Conference on Intelligent Robotics and Applications (ICIRA)*, Shanghai, China. November 10-12, 2010.

[6] G. Saur, S. Estable, K. Zielinski, S. Knabe, M. Teutsch, M. Gabel, "Detection and Classification of manmade Offshore Objects in TerraSAR-X and RapidEye Imagery: Selected Results of the DeMarine-DEKO Project", in *Proc. of IEEE OCEANS*, Santander, Spain, June 6-9, 2011.

[7] J. Cha, R. H. Cofer, S. P. Kozaitis, "Extended Hough transform for linear feature detection", *Pattern Recognition*, vol. 39, issue 6, 2006.

[8] M. C. K. Yang, J.-S. Lee, C.-C. Lien, C.-L. Huang, "Hough Transform Modified by Line Connectivity and Line Thickness", *IEEE Transactions on Pattern Analysis and Machine Intelligence*, vol. 19, no. 8, August 1997.

[9] V. Kamat, S. Ganesan, "A robust Hough transform technique for description of multiple line segments in an image", in *Proceedings of the 1998 International Conference on Image Processing (ICIP)*, Chicago, IL, USA, October 4-7, 1998.

[10] S. Du, B. J. van Wyk, C. Tu, X. Zhang, "An Improved Hough Transform Neighborhood Map for Straight Line Segments", *IEEE Transactions on Image Processing*, vol. 19, no. 3, March 2010.

[11] J. Li, Z. Long, Y. Li, R. Tang, "A Modified Segmentation Algorithm for Infrared Image", in *Proceedings of the 2010 International Conference on Optoelectronics and Image Processing (ICOIP)*, Haiko, Hainan, China, November 11-12, 2010.

[12] D. Fu, X. Wang, X. Han, "An Extraction of Infrared Occluded-object Based On Maximum Variance and Negative Selection", in *Proceedings of the 2008 International Workshop on Education Technology and Training & 2008 International Working on Geoscience and Remote Sensing*, Shanghai, China, December 21-22, 2008.

[13] P. Subashini, M. Krishnaveni, S. Kumar Thakur, "Coupling optimal method of segmentation with restoration for target detection in SAR images", in *Proc. of The 2nd International Conference on Computer and Automation Engineering (ICCAE)*, Singapore, Febr. 26-28, 2010.

[14] D. J. Crisp, *The state-of-the-art ship detection in synthetic aperture radar imagery*, Research Report DSTO-RR-0272, Defence Science and Technology Organisation, Edinburgh, Australia, 2004.

[15] M. Gabel, *Untersuchung von Schiffssignaturen in TerraSAR-X-Bildern*, diploma thesis, Universität Karlsruhe (TU), Germany, 2009.

[16] B. Fardi, J. Dousa, W. Gerd, B. Elias, A. Barke, "Obstacle detection and pedestrian recognition using a 3D PMD camera", in *Proc. of 2006 IEEE Intelligent Vehicles Symposium*, Tokyo, Japan, June 13-15, 2006.

[17] T. Schamm, J. M. Zöllner, S. Vacek, J. Schröder, R. Dillmann, "Obstacle detection with a photonic mixing device-camera in autonomous vehicles", *International Journal of Intelligent Systems Technologies and Applications*, vol. 5, pp. 315–324, November 2008.

[18] R. Labayrade, D. Aubert, J.-P. Tarel, "Real time obstacle detection in stereovision on non flat road geometry through "v-disparity" representation", in *Proceedings of the 2002 IEEE Intelligent Vehicle Symposium*, pp. 646–651, Versailles, France, June 17-21, 2002.

[19] Z. Hu, F. Lamosa, K. Uchimura, "A complete u-v-disparity study for stereovision based 3d driving environment analysis", in *Proceedings of the Fifth International Conference on 3-D Digital Imaging and Modeling (3DIM)*, pp. 204–211, Ottawa, Canada, June 13-16, 2005.

[20] G. Saur, M. Teutsch, "SAR signature analysis for TerraSAR-X-based ship monitoring", in *Proc. of SPIE Vol. 7830, Image and Signal Processing for Remote Sensing*, Toulouse, France, Sept. 20-22, 2010.